Optics & Laser Technology 181 (2025) 111994

Contents lists available at ScienceDirect

Optics and Laser Technology

journal homepage: www.elsevier.com/locate/optlastec

Full length article

Performance investigation of pre-ablation and reheating orthogonal double-pulse nanoparticle enhanced laser-induced breakdown spectroscopy

Junjuan Shang [a,e], Mengmeng Sun [a,c], Hongfang Song [b], Junya Ma [a], Wei Zhang [a,e], Huinan Huang [a], Zhihua Yuan [a], Jiandong Hu [a,e,*], Mengjiao Zhang [d,**], Muhammad Awais [a,e]

[a] College of Mechanical and Electrical Engineering, Henan Agricultural University, Zhengzhou 450001, Henan, China
[b] School of Science, Huzhou University, Huzhou 313000, Zhejiang, China
[c] Zhengzhou City Rail Transit Specialized Secondary School, Zhengzhou 450001, Henan, China
[d] College of Science, Henan Agricultural University, Zhengzhou 450001, Henan, China
[e] Henan International Joint Laboratory of Laser Technology in Agriculture Sciences, Zhengzhou 450001, Henan, China

ARTICLE INFO

Keywords:
DP-NELIBD
Relative standard deviation
Au nanoparticle
Signal-noise ratio
Spectral intensity

ABSTRACT

In this study, we propose a approach that nanoparticles enhanced double-pulse laser-induced breakdown spectroscopy (DP-LIBS). We also compare the effects of nanoparticles on pre-ablation and reheating orthogonal DP-LIBS. The aim is to improve the sensitivity, signal-to-noise ratio (SNR), and repeatability of LIBS emission spectra, which are inadequate for detecting of complex matrix samples. Gold nanoparticles (AuNPs) are synthesized chemically. The spacing between particles,which significantly influences spectral enhancement, is controlled by adjusting the AuNPs solution concentration applied to the Al surface. The optimal concentration is determined to be 0.168 mg/ml. We examined the impact of laser pulse energy, the interval delay time between two laser pulses, and detector gate delay time on the enhancement effect. Under optimum conditions, The SNR and Relative Standard Deviation (RSD) of both DP-NELIBS and DP-LIBS are Evaluated. Our findings real that reheating DP-LIBS, in the presence of AuNPs, results in a 1.5-fold to 3-fold increase in enhancement effects, and a 29% improvement in SNR. However, the presence of NPs in the pre-ablation structure slightly reduces performance. Overall, reheating DP-NELIBS can enhance sensitivity and lower detection limits through nanoparticle methods, thereby improving the accuracy of complex matrix samples.

1. Introduction

Laser-induced breakdown spectroscopy (LIBS) is a technique for qualitative and quantitative analysis of material and elemental by monitoring the positions and intensities of elemental-specific lines emitted from plasma during decay processes. Compared with other analytical techniques, LIBS stands out for its rapid, almost nondestructive, remote and multi-element analysis capabilities. These characteristics make LIBS highly valuable in various fields, including agriculture [1], industry [2], food [3], biology [4], and medicine [5]. However, LIBS has notable drawbacks, such as low precision and poor repeatability [6]. In order to improve LIBS performance, several methods have been proposed, such as double-pulse LIBS [7], plasma confined [8], microwave enhancement [9], spark discharge [10], target modification [11], ambient gas optimization [12], and nanoparticle enhancement [13]. Additionally, combining two or more methods has been studied for further improve LIBS, such as double-pulse-nanoparticle [14], spatially confined-spark discharge [15], spark-nanoparticle [16], magnetic field confined-nanoparticle [17], double pulse-spatially with N_2[6], spatially-
magnetic confined [18], and spatially confined-nanoparticle LIBS [19].

Recently, there has been increased attention on the combination of DP-LIBS and NELIBS techniques, showing remarkable improvements LIBS signals sensitivity. Fan Yang et al. [20] combined NELIBS and collinear DP-LIBS [4] on crystal SiO_2 demonstrating its enhancement effect. Au NPs films were deposited on crystal SiO_2 by thermal dewetting revealing that interparticle distance and size distribution affect LIBS spectral intensity. A 7.5 nm Au film showed the best effect on Si I intensity, achieving an enhancement factor of about 13 with NELIBS and 30 with DP-NELIBS [20]. F. Poggialini et al. [14] reported

* Correspondence to: College of Mechanical and Electrical Engineering, Henan Agricultural University, China.
** Corresponding author.
E-mail addresses: jiandonghu@163.com (J. Hu), zhangmengjiao@henau.edu.cn (M. Zhang).

https://doi.org/10.1016/j.optlastec.2024.111994
Received 12 August 2024; Received in revised form 24 September 2024; Accepted 18 October 2024
Available online 30 October 2024

using two parallel non-collinear laser pulses combined with NELIBS, named spatially offset DP-NELIBS (SO-DP-NELIBS), for collective signal enhancement. The best enhancement effect was observed with 0.5 mm distance between the two parallel laser pulses, achieving 10 folds enhancement compared to single laser pulse LIBS.

These studies primarily focus on the combination of collinear DP-LIBS and NELIBS to enhance LIBS signals. However, few experimental studies have investigated the combination of orthogonal DP-LIBS [21] and NELIBS, as well as comparisons between pre-ablation [22] DP-NELIBS and reheating [23] DP-NELIBS. Additionally, research on the signal-to-noise ratio and repeatability of LIBS emission spectra in orthogonal DP-NELIBS is limited, despite these being crucial factors in sample detection.

This article investigates the combination of NELIBS and orthogonally DP-LIBS on Aluminum alloy. Gold nanoparticles (15 nm in diameter) with various concentrations are deposited on the sample surface to determine the optimal particle concentration and to assess the effects of NPs. The study examines the influence factors such as delay time, laser pulse energy, and the interval time between two laser pulses on the enhancement of the spectra at Al II 199.05 nm, Al I 226.91 nm, Al I 257.51 nm, Al I 394.40 nm, and Al I 396.15 nm. Signal-to-noise ratio (SNR) and relative standard deviation (RSD) are also discussed under the optimized conditions. The performance of pre-ablation DP-NELIBS is compared with reheating DP-NELIBS, with results indicating that the presence of nanoparticles has a more pronounced effect in reheating DP-NELIBS.

2. Materials and methods

2.1. Experimental set-up

Fig. 1 illustrates the schematic diagram of the LIBS system used in this study. The experimental setup consists two Nd:YAG pulsed lasers (Grace Laser, model number: HASOR-400), each with a central wavelength of 1064 nm and a pulse duration of 7 ns. These lasers can deliver pulses with energies up to 400 mJ, and their repetition rate can be adjusted from a single shot up to 10 Hz. The laser beams have a close-to-Gaussian profile with a beam diameter of 7 mm. In this setup, one laser (laser 1) is directed perpendicular to the sample surface and tightly focused using a lens (focal length: 100 mm, diameter: 25.4 mm) to ablate the material. The second laser (laser 2) is also focused and aligned parallel to the sample surface, positioned approximately 1 mm above it. To control the ablation positions, the sample is mounted on a three-dimensional platform that can be adjusted as needed.

The plasma emission generated during the ablation process is collected and recorded using a compact eight-channel spectrometer (Ocean Optics, MX2500+). This spectrometer has a wavelength range of 180–1100 nm and a spectral resolution of 0.1 nm. The synchronization between the spectrometer and the lasers is managed by utilizing the Q-switch signal of the lasers. During spectral data collection, an integration time of 2 ms is selected. The spectral data is then transferred to a personal computer for further processing and analysis.

2.2. Sample preparation

Metallic Al thin plates, 2 mm thick, are collected from Anhui Zhengying Technology Co., Ltd.(Anhui, China). These plates contain Fe, Cu, Mn, Mg, Si, Zn, Cr and Ti, with an Al purity of 98.6%. The spectral lines selected for analysis include Al II 199.05 nm, Al I 226.91 nm, Al I 257.51 nm, Al I 394.40 nm, and Al I 396.15 nm, as listed in Table 1. Chloroauric acid tetrahydrate ($HAuCl_4 \cdot 4H_2O$) is purchased from Aladdin Reagents Co., Ltd. (Shanghai, China), and sodium citrate ($Na_3C_6H_5O_7 - 2H_2O$) is purchased from Sigma-Aldrich (USA). All solutions are prepared using pure water (Wahaha Group Co,. Ltd).

Table 1
Spectral parameters of Al.

Atom line	Wavelength (nm)	Intensity
Al II	199.05	700
Al I	226.91	50
Al I	257.51	800
Al I	394.40	500
Al I	396.15	1000

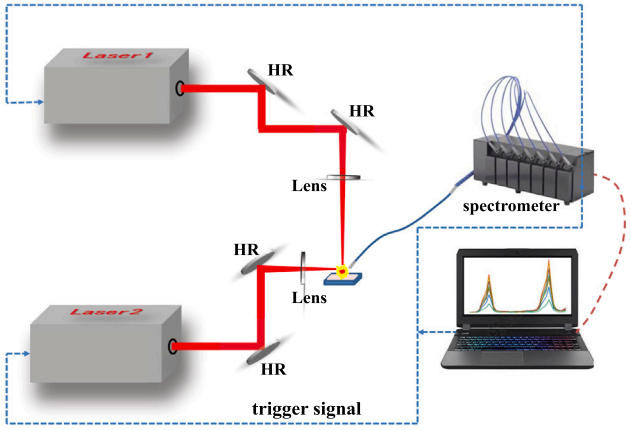

Fig. 1. Schematic diagram of DP-NELIBS experimental setup. HR: High reflection mirror.

The synthesis of AuNPs is accomplished by citrate reduction method [24]. The produced NPs are ultrapure and do not require any chemical stabilizers. Briefly, a conical flask containing 50 ml of ultrapure water is placed on a magnetic stirrer and continuously stirred at 150 °C. Then, 1.25 ml 0.4% $HAuCl_4$ is added to the conical flask. After boiling for 2 min, 1 ml sodium citrate solution (1% mass fraction) is quickly added and the stirring rate is increased. The solution's color gradually changed from light yellow to grey-black and finally maroon upon the addition of the sodium citrate solution. The mixture is heated for an additional 6 min after the color stabilized, and then allowed to cool to room temperature. The resulting AuNPs had a concentration of approximately 0.056 mg/ml and a size of approximately 15 nm, as previously described [24].

For the experiment, different concentrations of AuNPs (0.028, 0.056, 0.112, 0.14, 0.168, 0.2, 0.24, 0.28, 0.336 mg/ml) are prepared. AuNPs solutions with concentrations higher than 0.056 mg/ml are obtained by centrifuging the 0.056 mg/ml nanoparticle solution to eliminate the supernatant, followed by 5 min of ultrasound sonication. The 0.028 mg/ml AuNPs are obtained by diluting the 0.056 mg/ml nanoparticle solution with the corresponding purified water.

3. Results and discussion

3.1. The effects of nanoparticles concentration

To investigate the enhancement effect of the AuNPs concentration, nine different concentrations ranging from 0.028 to 0.336 mg/ml are utilized. Prior to ablation, a 1 μL droplet of the AuNPs solution is deposited on the surface of an Al plate, ensuring the solution spread evenly. The NPs are then allowed to air-dried naturally. Meanwhile, the laser pulse energies, delay times and interval delay times for reheating DP-NELIBS are set at 52 mJ, 76 mJ, 2.3 μs and 0.1 μs respectively. For pre-ablation DP-NELIBS, these parameters are set at 38.69 mJ, 89 mJ, 1.5 μs and 6 μs. The spectral intensity of the Al I 396.15 nm line is used for comparison, and the spectral data are averaged over 5 repeated experiments for each case.

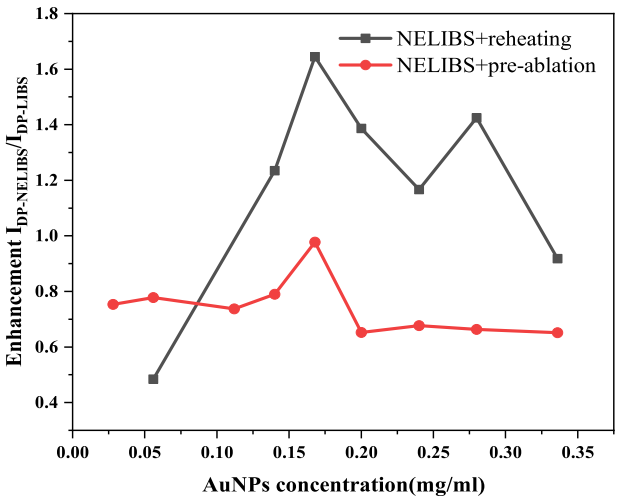

Fig. 2. Enhancement factor at various AuNPs concentrations.

The results, shown in Fig. 2, demonstrate that an AuNPs concentration of 0.168 mg/ml exhibits the highest enhancement factor. The enhancement effect of DP-NELIBS compared to DP-LIBS is approximately 0.98-fold (1.64-fold) for the pre-ablation (reheating) method, with lesser enhancements observed at other AuNPs concentrations. The significant enhancement by AuNPs is mainly attributed to the surface plasmon effect, which is generated under laser irradiation [25]. The surface plasmon effect strengthens the local electric field, and its magnitude strongly depends on the interparticle distance and NP sizes, as demonstrated in a previous work [13]. In this work, the optimal AuNPs concentration for enhancement is clearly determined to be 0.168 mg/ml.

3.2. Improvement in sensitivity

The effects of two laser interval delay time, laser pulse energy, and detector gate delay on the spectral intensity in DP-NELIBS are investigated. This effect is quantified by the enhancement ratio, $I_{DP-NELIBS}/I_{LIBS}$. It represents the ratio of the spectral intensities obtained using the DP-NELIBS and conventional LIBS methods, with each spectrum averaged over 5 accumulations.

In this study, both pre-ablation and reheating DP-NELIBS methods are examined and the compared with single pulse LIBS. The interval delay time between the two lasers pulse is investigated for its influence on plasma emission enhancement. Fig. 3 shows the relationship between spectral intensity enhancement effect and interval delay time. In the pre-ablation configuration (Fig. 3(a)), as the interval delay time increases, the signal rapidly surges until it reaches a maximum at 6 μs, and then gradually decreases. The variation in signal intensity with interval delay time is influenced by factors such as environmental temperature and pressure, mass removal rate, and plasma temperature [26]. As the interval delay time further increases, the ambient gas temperature and pressure gradually return to their normal values, resulting in a decrease in signal intensity. This observation is consistent with other reported results [7].

In the reheating configuration (Fig. 3(b)), the signal increases with increasing interval delay time until it reaches a maximum at 0.1 μs, after that it sets to decrease. This is because at an interval delay time of 0.1 μs, the plasma exhibits high electron density and temperature. Subsequently, the cooling down of plasma leads to a dramatic reduction in the density of electrons, ions and atoms in plasma plume.

In the next set of experiments, the laser energies are adjusted to achieve the strongest spectral emission signal intensity. LIBS and DP-NELIBS emission spectra are measured under the same laser 1 pulse energy. Fig. 4(a), (b), (c) and (d) illustrate the effect of laser pulse energy on the enhancement of emission line intensities at a fixed AuNPs concentration of 0.168 mg/ml. The results indicate that all spectral lines display a similar trend with laser pulse energy. At low laser pulse energy, the enhancement effects rapidly increase up to a maximum, after which they gradually decrease and level off. In the pre-ablation configuration, the optimized energies for laser 1 and laser 2 are found to be 55.8 mJ and 93.3 mJ, respectively. In the reheating configuration, the optimized energies are 42.2 mJ and 93.3 mJ. As mentioned above, the dominant ionization mechanism, influenced by nanoparticle-induced surface plasmon, is responsible for the enhancement in DP-NELIBS. At excessively high laser 1 pulse energy, the electromagnetic field enhancement with surface plasmon in DP-NELIBS weakens, leading to a reduction in the enhancement effect. This conclusion is consistent with the findings of Fan Yang et al. [20].

The spectral intensity of LIBS is known to yield quick-decaying. Therefore, the detector gate delay of the spectrometer is also optimized to enhance the emission spectra at the optimized laser pulse energy and NPs concentration. Fig. 4(e) and (f) plot the Al signal intensity enhancement as a function of the delay time. Each point on the graph represents the average of 10 laser events. The trends for each the spectrum are similar, with an initial increase followed by damping. The maximum enhancement effect is achieved at a delay time of about 1.8 μs for pre-ablation DP-NELIBS and 1.5 μs for reheating DP-NELIBS. This can be explained by the fact that plasma excitement takes a certain amount of time to reach its excited state and decays after reaching a maximum [27].

3.3. Spectral intensity enhancement by combining AuNPs and double-pulse

Fig. 5 shows the spectra for LIBS of Al II 199.05 nm, Al I 226.91 nm, Al I 257.51 nm, Al I 394.40 nm, and Al I 396.15 nm under different conditions. In pre-ablation LIBS configuration, the pulse energies of laser 1 and laser 2 are 55.8 mJ and 93.3 mJ, respectively. In the reheating LIBS configuration, the pulse energies are 42.2 mJ and 93.3 mJ. These pulse energies result in the highest spectral enhancement factors. The interval delay times for the two methods are 6 μs and 0.1 μs, and the delay times are 1.8 μs and 1.5 μs, respectively. Each measurement is repeated 100 times, and an average is calculated from 10 spectra to yield 10 spectral data points. Subsequently, the averages and the error bars for the enhancement factors of these 10 data points are determined. Fig. 5(a) and (b) represent the spectra obtained in pre-ablation and reheating configurations.

The enhancement ratios of pre-ablation DP-LIBS and reheating DP-LIBS with and without AuNPs are shown in Fig. 5(c). The figure illustrates that the enhancement factor decreased from about 7 times with pre-ablation DP-LIBS to about 5 times with addition of AuNPs. The exact mechanism behind this observation needs further experimental and theoretical investigations.

In contrast to pre-ablation DP-NELIBS, reheating DP-NELIBS exhibits significant enhancement in the line intensity for most transition lines, except for the Al II 199.05 nm transition line. The enhancement factor for these lines increases by 52% compared to reheating DP-LIBS. However, for Al II 199.05 nm, the spectral intensity of reheating DP-LIBS with and without AuNPs is nearly the same. The optimal conditions for the ablation of ionic spectral lines and atomic spectral lines may be different. In this experiment, the conditions, including laser pulse energies, delay times, interval times, and nanoparticle concentration, are all optimized based on the Al I 396.15 nm line. Therefore, the Al II line is unable to exhibit the enhancement effect with AuNPs. Further experimental research and in-depth exploration are still needed to provide more conclusive evidence.

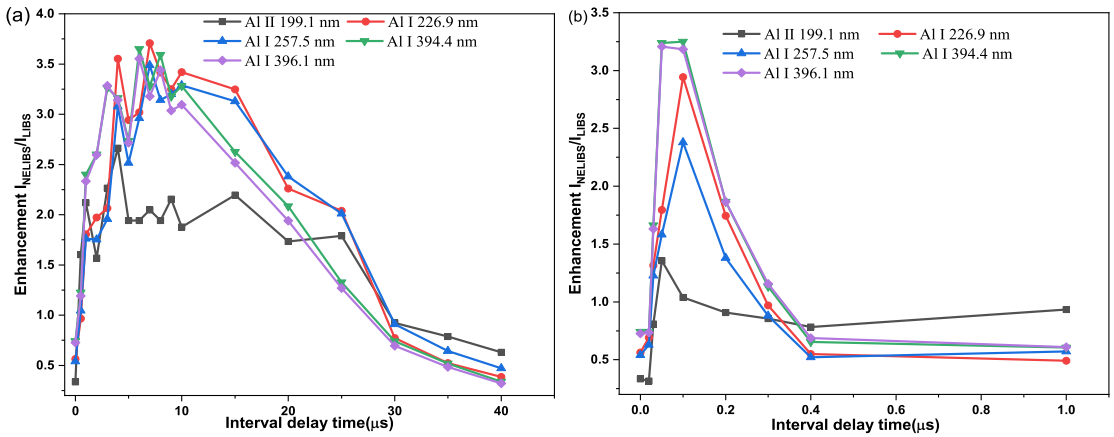

Fig. 3. Influence of the interval delay time between two lasers on the enhancement effects of NELIBS compared to LIBS: (a) Pre-ablation DP-NELIBS (b) Reheating DP-NELIBS.

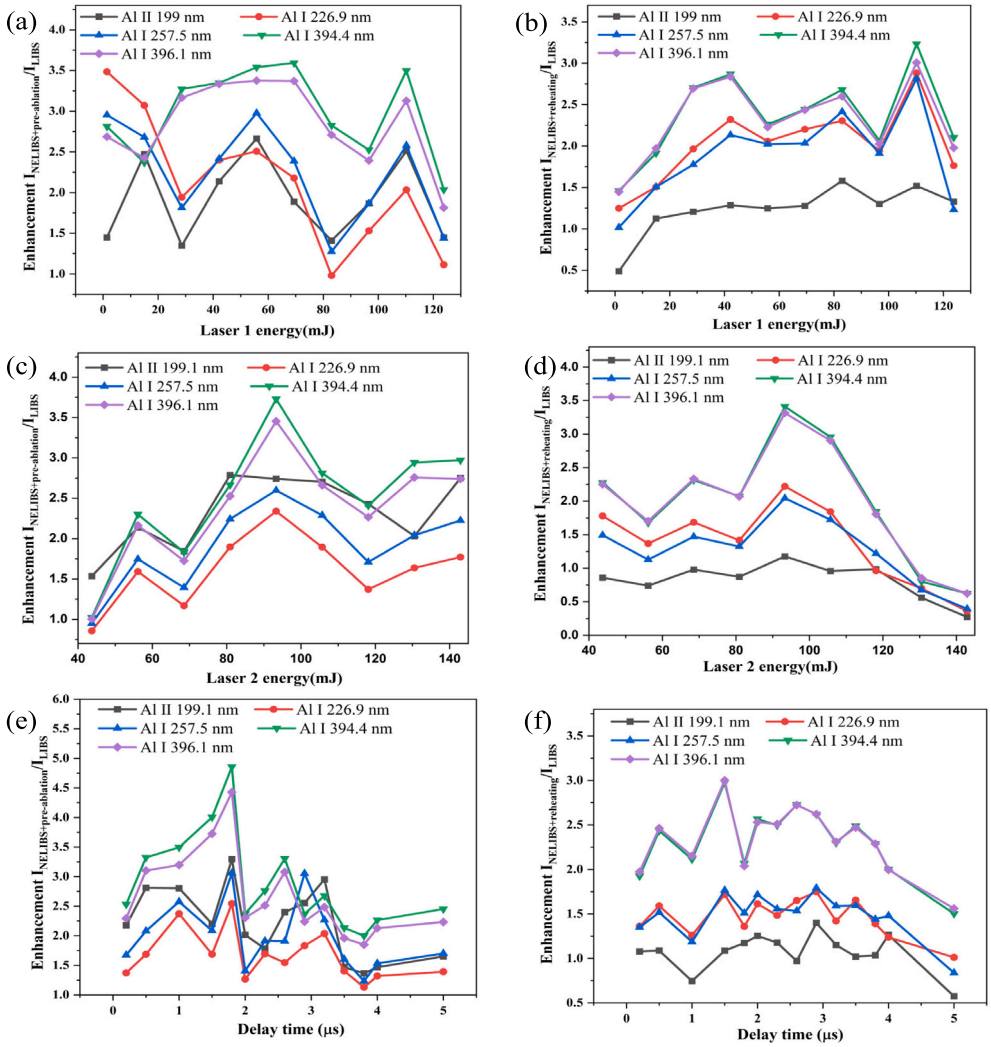

Fig. 4. Variation in spectral signal enhancement for emission lines of Al I and Al II. (a) and (b): laser 1 pulse energy; (c) and (d): laser 2 pulse energy; (e) and (f): detector gate delay time.

3.4. Comparison of RSD and SNR of spectral intensity

In order to compare the characteristics of pre-ablation DP-LIBS and reheating DP-LIBS with and without AuNPs, the RSD and SNR of the spectral intensity are analyzed. The selected spectral lines for analysis are Al II 199.05 nm, Al I 226.91 nm, Al I 257.51 nm, Al I 394.40 nm, and Al I 396.15 nm. All spectral intensities are measured under optimal conditions with laser 1 pulse energy of 55.8/42.2 mJ, laser 2 pulse

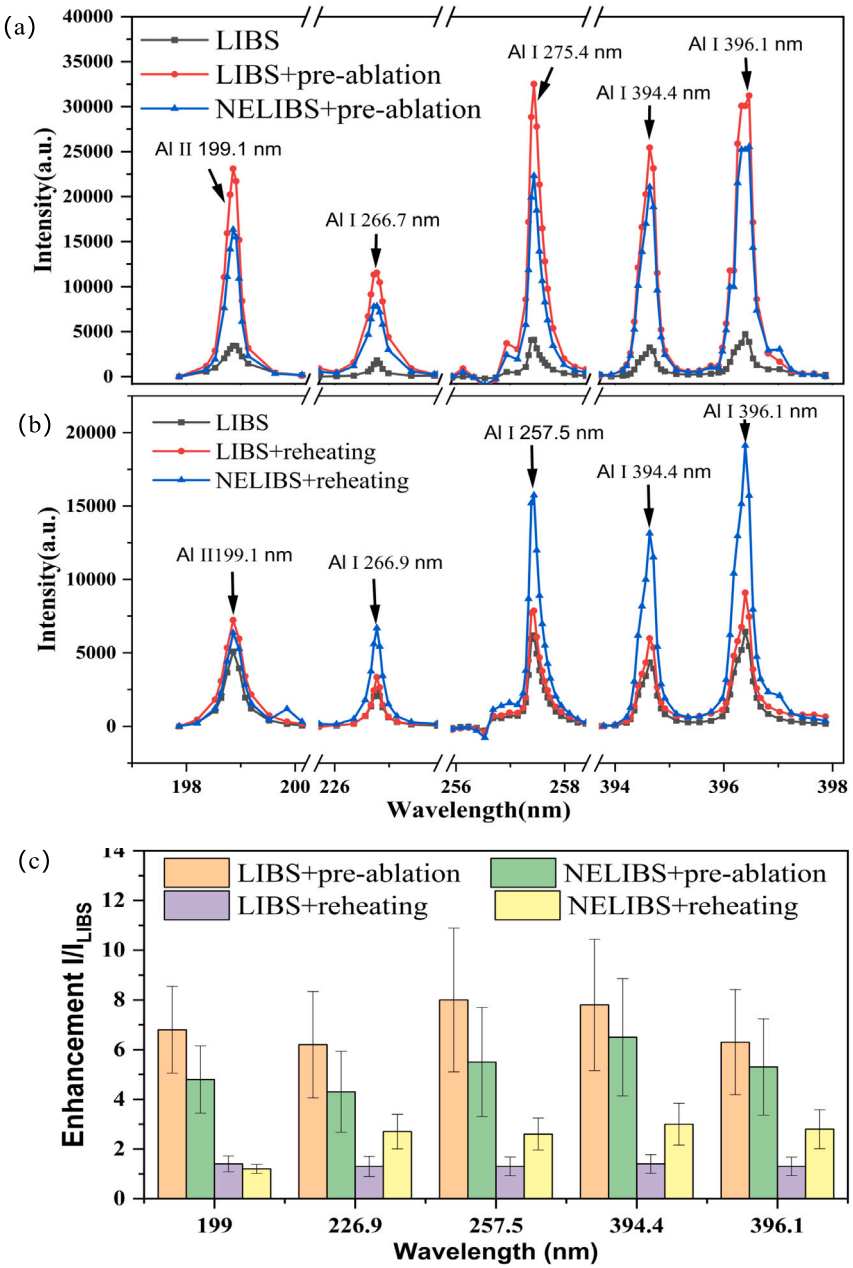

Fig. 5. Spectra for LIBS of Al II 199.05 nm, Al I 226.91 nm, Al I 257.51 nm, Al I 394.40 nm, and Al I 396.15 nm under different conditions: (a) Pre-ablation LIBS method, (b) Reheating LIBS method and (c) enhancement effect of spectral intensity.

energy of 93.3/93.3 mJ, AuNPs concentration of 0.168/0.168 mg/ml, interval time delay between two lasers of 6/0.1 μs, and gate delay time of 1.8 μs/1.5 μs for pre-ablation/reheating DP-NELIBS. The methods for spectral acquisition and data processing are consistent with those used for the enhancement factor.

The stability of spectral intensity measured by the RSD, is shown in Fig. 6(a). In pre-ablation DP-LIBS with AuNPs, the RSD increase by 11.8–184.6%. The increase in RSD can be attributed to the non-homogeneous distribution of NPs on the sample surface, introducing additional variability in the measurements [28].

In contrast, the RSD in the reheating DP-LIBS configuration exhibited different trends for different spectral lines when NPs are deposited on the Al surface. Specifically, the RSD decreases by 25%, 27% and 84% for the Al II 199.05 nm, Al I 226.91 nm, and Al I 257.51 nm lines, respectively. Conversely, it increases by 35% and 42% for Al I 394.40 nm and Al I 396.15 nm lines. These observations suggest that the distribution of laser energy may vary across different wavelengths.

Fig. 6(b) represents the SNR of the spectra. In pre-ablation DP-LIBS, the addition of NPs slightly increased the SNR of the Al II 199.05 nm spectral line, while the SNR of other atomic spectral lines is not significantly affected. This indicate that, within the error range, the SNR of pre-ablation DP-LIBS is not substantially influenced by the presence of NPs. However, in the case of reheating DP-LIBS, the addition of NPs resulted in a 29% increase in the spectral SNR. Notably, the SNR enhancement ratios are lower than the intensity enhancement ratios observed previously. Suggesting that NPs may enhance the noise as well as the signal in the spectrum [28]. This could be attributed to thermal effects, scattering effects, or other interactions between the NPs and the sample.

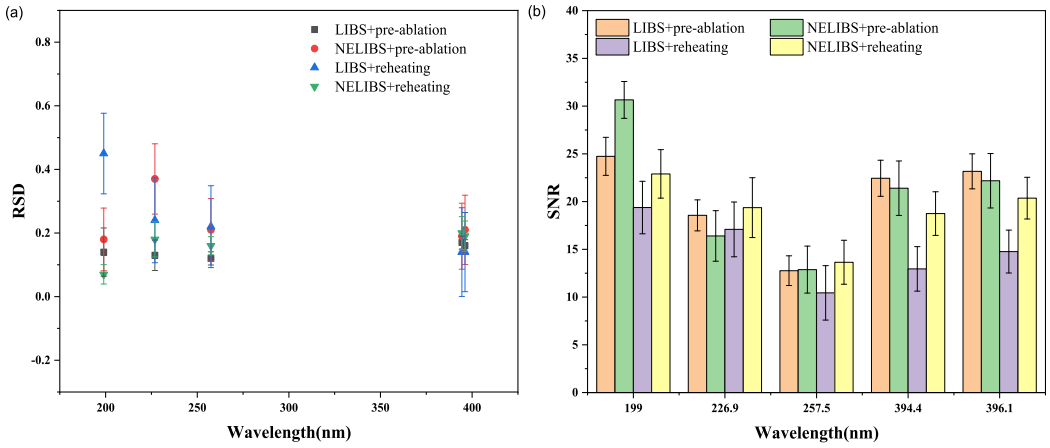

Fig. 6. Comparison of (a) RSD and (b) SNR measured in DP-LIBS and DP-NELIBS at the optimized conditions, including laser pulse energies, AuNPs concentration, detector gate delay time and interval delay time between two lasers.

4. Conclusion

In this study, we proposed a novel approach that combines orthogonal double-pulse laser-induced breakdown spectroscopy with nanoparticle enhanced LIBS to improve the LIBS performances. The two configurations of pre-ablation DP-NELIBS and reheating DP-NELIBS are discussed.

The effect of AuNPs concentration on the enhancement of DP-LIBS is studied. The results show that the enhancement effect of DP-NELIBS strongly depended on the AuNPs concentration, with 0.168 mg/ml yielding the best enhancement effect. Laser pulse energies, interval delay time between two laser pulses, and detector gate delay times are optimized to improve the enhancement effect. All spectral intensities are measured under optimal conditions with laser 1 pulse energy of 55.8/42.2 mJ, laser 2 pulse energy of 93.3/93.3 mJ, AuNPs concentration of 0.168/0.168 mg/ml, interval delay times between the two lasers of 6/0.1 μs, and gate delay times of 1.8 μs/1.5 μs for pre-ablation/reheating DP-NELIBS.

In addition, we also compared the characteristics of pre-ablation DP-NELIBS and reheating DP-NELIBS in terms of spectral intensity enhancement effect, SNR and RSD. When AuNPs are added, the enhancement effect of pre-ablation DP-LIBS diminishes. whereas, reheating DP-LIBS shows a twofold improvement in spectral intensity. The RSD of pre-ablation DP-NELIBS increases by 11.8% to 184.6% compared to pre-ablation DP-LIBS, indicating decreased repeatability of spectral line intensity. In contrast, for reheating DP-NELIBS, the RSD of certain spectral lines is lower, while for others, it is higher than reheating DP-LIBS. The addition of AuNPs silently influences the SNR of spectral intensity in pre-ablation DP-LIBS. However, in reheating DP-NELIBS, the SNR increases by 29%. In summary, AuNPs improve the characteristics of reheating DP-LIBS but have a silent impact on pre-ablation DP-LIBS. The combination of DP-LIBS and NELIBS is worthy of further investigation for material and element qualitative and quantitative analysis.

CRediT authorship contribution statement

Junjuan Shang: Writing – review & editing, Investigation, Conceptualization. **Mengmeng Sun:** Writing – original draft, Data curation. **Hongfang Song:** Writing – review & editing. **Junya Ma:** Data curation. **Wei Zhang:** Writing – review & editing. **Huinan Huang:** Writing – review & editing. **Zhihua Yuan:** Writing – review & editing, Project administration. **Jiandong Hu:** Writing – review & editing, Project administration. **Mengjiao Zhang:** Writing – review & editing, Supervision. **Muhammad Awais:** Writing – review & editing.

Declaration of competing interest

The authors declare that they have no conflict of interest for this work.

Acknowledgments

This work was supported by the Henan Provincial Science and Technology Research Project (No. 242102321075) and Key Research Projects of Higher Education Institutions in Henan Province (No. 25B41 6008).

Data availability

Data will be made available on request.

References

[1] R. Zhou, K. Liu, Z. Tang, Z. Hao, X. Li, X. Zeng, Determination of micronutrient elements in soil using laser-induced breakdown spectroscopy assisted by laser-induced fluorescence, J. Anal. At. Spectrom. 36 (3) (2021) 614–621.
[2] Z. Wang, Y. Deguchi, F. Shiou, S. Tanaka, M. Cui, K. Rong, J. Yan, Feasibility investigation for online elemental monitoring of iron and steel manufacturing processes using laser-induced breakdown spectroscopy, ISIJ Int. 60 (5) (2020) 971–978.
[3] D. Stefas, N. Gyftokostas, P. Kourelias, E. Nanou, C. Tananaki, D. Kanelis, V. Liolios, V. Kokkinos, C. Bouras, S. Couris, Honey discrimination based on the bee feeding by laser induced breakdown spectroscopy, Food Control 134 (3) (2022) 108770.
[4] J. Ren, Z. Yang, Y. Zhao, K. Yu, Collinear double-pulse laser-induced breakdown spectroscopy based Cd profiling in the soil, Opt. Express 30 (21) (2022) 37711–37726.
[5] J. Wang, X. Li, P. Zheng, S. Zheng, X. Mao, H. Zhao, R. Liu, Characterization of the Chinese traditional medicine artemisia annua by laser-induced breakdown spectroscopy (LIBS) with 532 nm and 1064 nm excitation, Anal. Lett. 53 (6) (2020) 922–936.
[6] H. Li, C. Wang, Y. Wang, S. Fu, L. Fang, Double-enhanced LIBS system with N_2 atmosphere and cylindrical cavity confinement for quantitative analysis of Sr element in soil, Meas. Sci. Technol. 34 (9) 095204, (8).
[7] N. Li, E. Harefa, W. Zhou, Nanosecond laser preheating effect on ablation morphology and plasma emission in collinear dual-pulse laser-induced breakdown spectroscopy, Plasma Sci. Technol. 24 (11) (2022) 115507.
[8] Q. Wang, A. Chen, D. Zhang, Y. Wang, L. Sui, S. Li, Y. Jiang, M. Jin, The role of cavity shape on spatially confined laser-induced breakdown spectroscopy, Phys. Plasmas 25 (7) (2018) 073301.
[9] A.F. Abu Kasim, M.A. Wakil, K. Grant, M. Hearn, Z.T. Alwahabi, Aqueous ruthenium detection by microwave-assisted laser-induced breakdown spectroscopy, Plasma Sci. Technol. 24 (8) (2022) 084004.
[10] Z. Ye, W. Ke, W. Wang, H. Yuan, X. Wang, X. Wang, D. Liu, A. Yang, M. Rong, Enhancement by spark discharge in LIBS detection of copper particle contamination in oil-immersed transformer, IEEE Trans. Dielectr. Electr. Insul. 29 (5) (2022) 2034–2041.

[11] Y. Jiang, Z. Lin, R. Li, Y. Chen, Improving the analytical sensitivity of orthogonal double-pulse laser-induced breakdown spectroscopy with target-enhancement, Spectrochim. Acta B 181 (2021) 106221.
[12] N. Giannakaris, A. Haider, C.M. Ahamer, S. Gruenberger, S. Trautner, J.D. Pedarnig, Femtosecond single-pulse and orthogonal double-pulse laser-induced breakdown spectroscopy (LIBS): Femtogram mass detection and chemical imaging with micrometer spatial resolution, Appl. Spectrosc. 76 (8) (2021) 926–936.
[13] Z. Salajkova, V. Gardette, J. Kaiser, M. Dell'Aglio, A. De Giacomo, Effect of spherical gold nanoparticles size on nanoparticle enhanced laser induced breakdown spectroscopy, Spectrochim. Acta B 179 (2021) 106105.
[14] F. Poggialini, B. Campanella, S. Legnaioli, S. Pagnotta, V. Palleschi, Investigating double pulse nanoparticle enhanced laser induced breakdown spectroscopy, Spectrochim. Acta B 167 (2020) 105845.
[15] Z. Hou, Z. Wang, J. Liu, W. Ni, Z. Li, Combination of cylindrical confinement and spark discharge for signal improvement using laser induced breakdown spectroscopy, Opt. Express 22 (11) 12909–12914.
[16] Q.-X. Li, D. Zhang, Y.-F. Jiang, S.-Y. Li, A.-M. Chen, M.-X. Jin, Combination of spark discharge and nanoparticle-enhanced laser-induced plasma spectroscopy, Chin. Phys. B 31 (8) (2022) 085201.
[17] X.-j. Hao, H.-j. Tang, X.-t. Hu, Detection sensitivity improvement study of LIBS by combining au-nanoparticles and magnetic field, Spectrosc. Spectr. Anal. 39 (5) (2019) 1599–1603.
[18] B.-H. Li, X. Gao, C. Song, J.-Q. Lin, Laser induced plasma spectral characteristics of Cu with magnetically and spatially combined confinement, Acta Phys. Sin. 65 (23) (2016) 235201.
[19] X. Hao, P. Sun, Y. Tian, B. Pan, Effect of plane mirrors combined with Au-nanoparticle confinement on the spectral properties of fe plasma induced by laser-induced breakdown, ACS Omega 7 (2022) 23605–23610.
[20] F. Yang, L. Jiang, S. Wang, Z. Cao, L. Liu, M. Wang, Y. Lu, Emission enhancement of femtosecond laser-induced breakdown spectroscopy by combining nanoparticle and dual-pulse on crystal SiO2, Opt. Laser Technol. 93 (2017) 194–200.
[21] P. Lu, Z. Zhuo, W. Zhang, T. Sun, J. Tang, J. Lu, Investigation of the secondary breakdown of double-pulse laser-induced breakdown spectroscopy with different focusing geometries and positions, J. Anal. At. Spectrom. 37 (11) (2022) 2320–2329.
[22] J. Uebbing, J. Brust, W.S.F. Leis, K. Niemax, Reheating of a laser-produced plasma by a second pulse laser, Appl. Spectrosc. 45 (9) (1991) 1419–1423.
[23] K.L.E. Dimitra N Stratis, S.M. Angel, Dual-pulse LIBS using a pre-ablation spark for enhanced ablation and emission, Appl. Spectrosc. 54 (9).
[24] S. Liu, J. Zhao, J. Wu, L. Wang, J. Hu, S. Li, H. Zhang, A deep learning-enabled smartphone platform for rapid and sensitive colorimetric detection of dimethoate pesticide, Anal. Bioanal. Chem. 415 (29–30) (2023) 7127–7138.
[25] R. Yi, J. Li, X. Yang, R. Zhou, H. Yu, Z. Hao, L. Guo, X. Li, X. Zeng, Y. Lu, Spectral interference elimination in soil analysis using laser-induced breakdown spectroscopy assisted by laser-induced fluorescence, Anal. Chem. 89 (4) (2017) 2334–2337.
[26] A. Safi, M. Bahreini, S.H. Tavassoli, Comparative study of two methods of orthogonal double-pulse laser-induced breakdown spectroscopy of aluminum, Opt. Spectrosc. 120 (3) (2016) 367–378.
[27] B. Lei, B. Xu, J. Wang, J. Li, Y. Wang, J. Tang, W. Zhao, Y. Duan, Time-resolved characteristics of laser induced breakdown spectroscopy on non-flat samples by single beam splitting, RSC Adv. 10 (65) (2020) 39553–39561.
[28] J. Liu, Z. Hou, T. Li, Y. Fu, Z. Wang, A comparative study of nanoparticle-enhanced laser-induced breakdown spectroscopy, J. Anal. At. Spectrom. 35 (10) (2020) 2274–2281.